Edge-Based FEM-BEM for Wide-Band Electromagnetic Computation

H. T. Yu[1], S. L. Ho[2], M. Q. Hu[1], and H. C. Wong[3]

[1]Department of Electrical Engineering, Southeast University, Nanjing 210096, China
[2]Department of Electrical Engineering, Hong Kong Polytechnic University, Kowloon, Hong Kong
[3]Industrial Centre, Hong Kong Polytechnic University, Kowloon, Hong Kong

Edge-based finite element method-boundary element method (FEM-BEM) for the computation of three-dimensional (3-D) electromagnetic fields at high and low frequencies is presented. A novel H–A model that includes the differential and integral equations for wide-band electromagnetic problems is described. An edge element method is implemented to discretize the proposed formulation. A surface edge element method (SEEM) for surface of arbitrary shape targets is derived according to the geometrical properties of the basis functions. Unlike traditional electromagnetic formulations, the major coefficients of the proposed formulation in this model are frequency independent and hence the model can be used to solve electromagnetic problems over a wide range of frequencies. The proposed method is implemented to compute: 1) the electromagnetic induction problems at low frequencies and 2) the scattering fields at high frequency. Results from established methods are used to validate the proposed method.

***Index Terms*—Edge-based FEM-BEM, electromagnetic induction, scattering field, surface edge element method.**

I. Introduction

THE edge element method (EEM) [1] was proposed by Nedelec in 1980. Only local elements are involved in such formulations and the tangential components of the vectors are continuous. Compared with the nodal-based finite element method (NBFEM), EEM needs fewer unknowns and hence is intrinsically more accurate. With EEM, the field vectors are used directly as variables. In NBFEM, one needs to compute, firstly, the potential which is an intermediate variable. Bossavit *et al.* [2], [7] have also implemented EEM to discretize FEM formulations for solving eddy-current problems at low frequency and scattering field at high frequency.

In addition to having the merits of edge elements, edge-based finite element method-boundary element method (FEM-BEM) can be used to solve electromagnetic (EM) problems in open areas and is more convenient to use when dealing with boundary conditions than in edge-based FEM with nodal-based BEM. Wakao *et al.* [3] also solve eddy-current problems of rectangular targets using edge-based FEM-BEM using hexahedron as the local element. Ahn solves high-frequency problems with a local tetrahedron element but the parameters in the expression of the surface basis function are not presented [4]. Moreover, the FEM-BEM formulation in [3] may not solve high-frequency EM problems because the effect of displacement current has been excluded. The coefficients in the electric field integral equation (EFIF) in [4] and (15) in [6] are frequency dependent. Such a coefficient in one field may become very dominant when the displacement current becomes negligible and the contribution of the other EM fields in the same formula could then be overshadowed. Daveau *et al.* [6] also mention that such formulations are not applicable readily at low frequency.

A novel edge-based FEM-BEM to study wide-band EM problems is proposed. **H**–**A** formulation based on the differential and integral equations is derived. A three-dimensional (3-D) edge element method is used to discretize the differentiation formulation. SEEM is derived and implemented to discretize the integral equation to facilitate the proposed FEM-BEM which is being used to solve arbitrarily shaped targets. The characteristics of the proposed formulation are that the coefficients of the discretized formulation are insensitive to frequencies and therefore it can be used to solve EM problems at high and low frequencies. Finally, the proposed FEM-BEM is used to solve EM induction (EM-I) problems and to compute the scattering fields. The computational results are validated by either experiments or other numerical methods.

II. Surface Edge Element Method

The 3-D edge element method has been widely used in FEM computation and its basis function for any order is well known. Hence, the following discussion will focus on SEEM for targets of arbitrate shapes. The surface basis functions of EEM for the FEM-BEM computations in [4] have been presented but the corresponding nodal basis function for surfaces of arbitrary shapes have not been presented. In this paper, the development of SEEM for arbitrary targets are discussed.

Assume an arbitrary point $P(x, y, z)$ in Fig. 1 is located inside a triangular patch $\Delta P_1 P_2 P_3$ on the surfaces of a general object without any of its sides parallel to the X, Y, or Z axis. The nodal basis function in this case is a linear function of coordinates and

$$\lambda_{si} = a_i + b_i x + c_i y + d_i z \tag{1}$$

where a_i, b_i, c_i, d_i are coefficients related to the size and shape of the triangle.

From the property of nodal basis function, one obtains

$$\begin{bmatrix} 1 & x_1 & y_1 & z_1 \\ 1 & x_2 & y_2 & z_2 \\ 1 & x_3 & y_3 & z_3 \\ 0 & n_x & n_y & n_z \end{bmatrix} \begin{Bmatrix} a_i \\ b_i \\ c_i \\ d_i \end{Bmatrix} = \begin{Bmatrix} k_{i1} \\ k_{i2} \\ k_{i3} \\ 0 \end{Bmatrix} \tag{2}$$

Digital Object Identifier 10.1109/TMAG.2006.871457

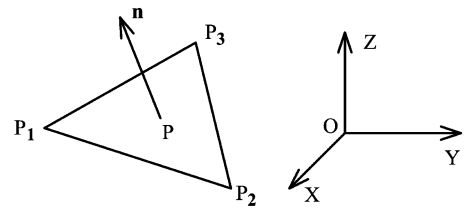

Fig. 1. Triangular patch.

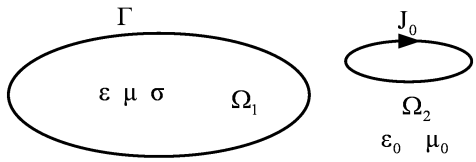

Fig. 2. Electromagnetic problem configuration.

where n_x, n_y, n_z are the three normalized components of a normal vector $\mathbf{n}$ of the plane $\Delta P_1P_2P_3$, $K_{ij} = 0$ if $i \neq j$, and $K_{ij} = 1$ if $i = j$. The first three equations are obtained based on the property of the nodal basis functions. The fourth row of (2) is obtained from the geometrical property of nodal basis function, and it is equivalent to the normalized plane equation enclosing the corresponding edge on a triangular patch. However, there are many such planes and hence the fourth row in (2) is imposed in order to select the plane, which is vertical to the local triangle patch, as the basis plane for which (1) has a unique solution.

Therefore, one of the edge based basis functions related to edge $e = \{i, j\}$ is obtained as follows:

$$\mathbf{N}_{se} = \lambda_{si}\nabla\lambda_{sj} - \lambda_{sj}\nabla\lambda_{si}. \tag{3}$$

As in volume edge elements, the following identity is always held:

$$\mathbf{N}_{se} \cdot \overrightarrow{ij} \equiv \pm 1 \tag{4}$$

which ensures that the tangential components of the vectors are always continuous between two adjacent elements.

The equivalent electrical and magnetic currents are related to the corresponding tangential magnetic and electric fields on the surface integration as follows:

$$\mathbf{J}_s = \sum_{e=1}^{3} \mathbf{J}_{se} = \sum_{e=1}^{3} \mathbf{n} \times \mathbf{H}_e = \sum_{e=1}^{3} \mathbf{n} \times \mathbf{N}_{se} H_e \tag{5}$$

$$\mathbf{M}_s = \sum_{e=1}^{3} \mathbf{M}_{se} = -\sum_{e=1}^{3} \mathbf{n} \times \mathbf{E}_e = -\sum_{e=1}^{3} \mathbf{n} \times \mathbf{N}_{se} E_e \tag{6}$$

where H_e is an edge variable corresponding to the magnetic density, E_e is the equivalent electric field. $\mathbf{n} \times \mathbf{N}_{se}$ is a constant in a direction normal to the edge $\overrightarrow{ij}$ such that the equivalent currents are continuous in the normal direction of the adjacent elements to satisfy the surface current properties.

III. Formulations

Fig. 2 shows the EM problem investigated in this paper. Ω_1 is a 3-D general target enclosed by the surface Γ, in which the parameters are: conductivity σ, permeability μ, permittivity ε. Ω_2 is the nonconducting region, where the parameters are: permeability μ_0, permittivity ε_0, and the current density in this region is $\mathbf{J}_0$.

A. Inside Targets

FEM is implemented inside the object and the magnetic field density vector $\mathbf{H}$ and magnetic potential vector $\mathbf{A}$ are set as physical variables. From Maxwell's equations, the following expressions are derived:

$$\nabla \times \mathbf{H} = (\sigma + j\omega\varepsilon)\mathbf{E} \tag{7}$$

$$\nabla \times \mathbf{E} = -j\omega\mathbf{B}. \tag{8}$$

Equations (7) and (8) can be rewritten as

$$\nabla \times \frac{1}{\sigma + j\omega\varepsilon} \nabla \times \mathbf{H} = -j\omega\mu\mathbf{H}. \tag{9}$$

Using vector identities, one obtains

$$\mathbf{W}_i \cdot \nabla \times \nabla \times \mathbf{H} = \nabla \times \mathbf{W}_i \cdot \nabla \times \mathbf{H} - \nabla \cdot (\mathbf{W}_i \times \nabla \times \mathbf{H}). \tag{10}$$

Setting

$$\mathbf{E} = -j\omega\mu_0\mathbf{A}_1 \tag{11}$$

where $\mathbf{A}_1 = \mathbf{A}^*/\mu_0, \mathbf{A}^*$ is the conventional reduced magnetic vector potential.

By adding (11), (9) can be changed into

$$\mathbf{W}_i \cdot \nabla \times \nabla \times \mathbf{H} = \nabla \times \mathbf{W}_i \cdot \nabla \times \mathbf{H} + j\omega\mu_0(\sigma + j\omega\varepsilon)\nabla \cdot (\mathbf{W}_i \times \mathbf{A}_1). \tag{12}$$

Integrating both sides of (12) gives the following governing equation:

$$\int_{\Omega_1} \nabla \times \mathbf{W}_e \cdot \nabla \times \mathbf{H} dV + j\omega\mu(\sigma + j\omega\varepsilon) \int_{\Omega_1} \mathbf{W}_e \cdot \mathbf{H} dV + j\omega\mu_0(\sigma + j\omega\varepsilon) \oint_{\Gamma} (\hat{\mathbf{n}} \times \mathbf{A}_1) \cdot \mathbf{W}_e dS = 0 \tag{13}$$

where $\mathbf{W}_e$ is the weighting function for the vector basis function $\mathbf{N}_e$, $\hat{\mathbf{n}}$ is the outward unit vector normal to the surface of the target.

By implementing 3-D EEM, the vector $\mathbf{H}$ is interpolated within a tetrahedron as follows:

$$\mathbf{H} = \sum_{e=1}^{6} \mathbf{N}_e H_e \tag{14}$$

where the vector basis function $\mathbf{N}_e$ for the volume edge element method is expressed as

$$\mathbf{N}_e = \lambda_i \nabla\lambda_j - \lambda_j \nabla\lambda_i \tag{15}$$

where λ_i is the 3-D nodal basis function.

As the third term in (13) exists only on the surface of targets, the surface basis function is used to interpolate A_1

$$\mathbf{n} \times \mathbf{A}_1 = \mathbf{n} \times \sum_{e=1}^{3} \mathbf{N}_{se} A_{1e} \tag{16}$$

where A_{1e} is an unknown, $\mathbf{N}_{se}$ stands for the surface basis function as shown in (3).

B. On the Surface of Targets

On the surface of targets, edge-based BEM is incorporated into the integral equation. The integral formulation for general targets in this region is derived from the Green's theorem

$$C_p \mathbf{H}_i = \int_{\Omega_s} \mathbf{J}_0 \times \nabla G d\Omega_s + j\omega\varepsilon_0 \oint_{\Gamma} (\hat{\mathbf{n}} \times \mathbf{E}) G dS' - \oint_{\Gamma} (\hat{\mathbf{n}} \times \mathbf{H}) \times \nabla G dS' - \oint_{\Gamma} (\hat{\mathbf{n}} \cdot \mathbf{H}) \nabla G dS'. \tag{17}$$

By setting $\hat{\mathbf{n}} \cdot \mathbf{H} = \hat{\mathbf{n}} \cdot \nabla \times \mathbf{A}_1$ and, together with (11), the governing function in this region can be rewritten as

$$C_p \mathbf{H}_i = \int_{\Omega_s} \mathbf{J}_0 \times \nabla G d\Omega_s + k_0^2 \oint_{\Gamma} (\hat{\mathbf{n}} \times \mathbf{A}_1) G dS' - \oint_{\Gamma} (\hat{\mathbf{n}} \times \mathbf{H}) \times \nabla G dS' - \oint_{\Gamma} (\hat{\mathbf{n}} \cdot \nabla \times \mathbf{A}_1) \nabla G dS' \tag{18}$$

where the constant C_p is dependent on the position of the field point, and $k_0 = \omega\sqrt{\mu_0\varepsilon_0}$ is the propagation constant in free space. G in (17) and (18) is the Green's function.

The first term on the right-hand side in (18) represents the driving source excited by the sensor and the second term stands for the contribution of displacement current, which can be neglected at low frequencies because k_0 is very small in this situation. Another feature of (18) is that the coefficients of the other two terms are fairly constant and are practically frequency independent.

Applying Galerkin method to (18) and setting the weighting function $\mathbf{W}_{se} = \hat{\mathbf{n}} \times \mathbf{N}_{se}$, one can obtain the linear equations for the surface of targets.

The application of $\mathbf{A}_1$ in (13) and (18) makes the values of coefficients corresponding to the $\mathbf{A}_1$ terms in (13) and (18) comparable to those of other terms, hence the characteristics of the discretized equations are significantly improved.

IV. Examples

A. EMI Response From a Cube

The first example used to test the proposed FEM-BEM method is to simulate the electromagnetic response from a conducting target. EM induction (EM-I) is widely used for the detection and discrimination of conducting and permeable targets using specific sensors. In the context of subsurface sensing, EM-I is used to simulate the signature of buried metal in land-mines and unexploded ordnance (UXO) [8]. As the conductivity of such targets is typically many orders of magnitude larger than that of the soil, the target can be analyzed with the assumption that it is located, approximately, in free space. The frequency-domain EM-I response of a conducting or ferrous target is characterized by the lowest resonant frequency at which the EM-I response is much stronger than that of other modes.

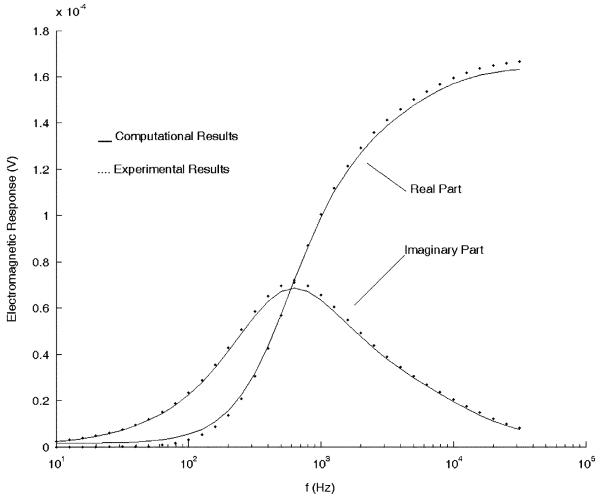

Fig. 3. Frequency feature of EMI response.

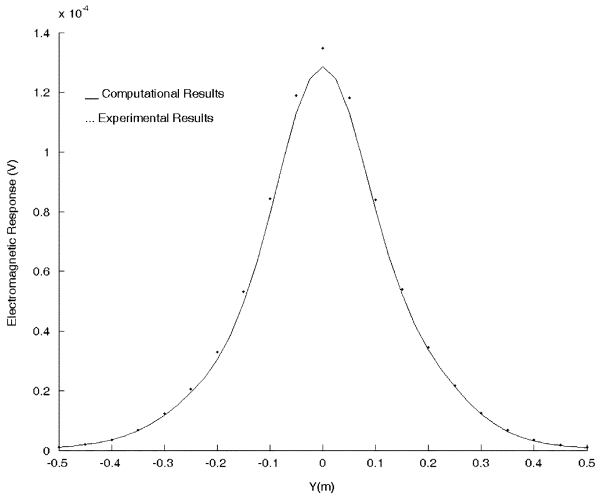

Fig. 4. Electromagnetic Induction responses along the Y-direction.

A numerical computation to investigate the EM-I response from a simple model in the form of a cube, 0.07 m on each side with a conductivity of 1.3×10^6 S/m is reported below. The distance between the cube and the sensor center is 0.2 m. The EM-I responses in the form of the terminal voltage at the end of the receiver over the frequency range of 10 Hz to over 10 kHz and with different distances between the sensor and the target are simulated by the proposed FEM-BEM method. Meanwhile, an experiment is carried out to validate the numerical results. In the experiment, the conducting cube is put on a plastic frame in order to reduce the environmental effects. The sensor includes the source and receiving coils. Due to the weakness of the response signal and as the source is very close to the receiver, one needs to detect the signal from the actual target and then the experiment is repeated again with the target removed in order to assess the environmental effects.

The results shown in Fig. 3 are divided into real and imaginary parts, and the imaginary part of the EM-I response is observed to reach its maximum when the frequency is close to the lowest resonant frequency. The real part of the EM-I response becomes larger as frequency increases but its incremental change will

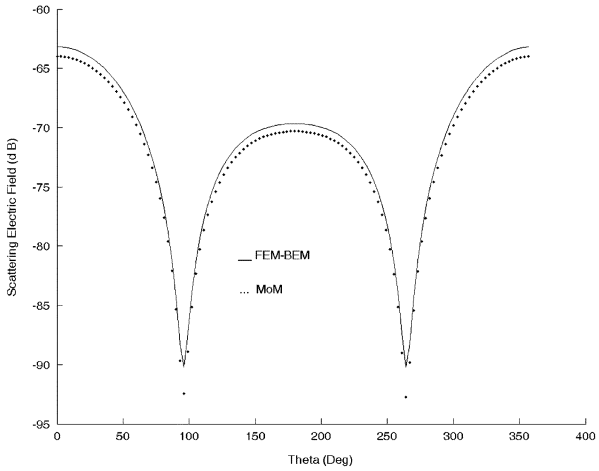

Fig. 5. Scattering field computed using two different methods.

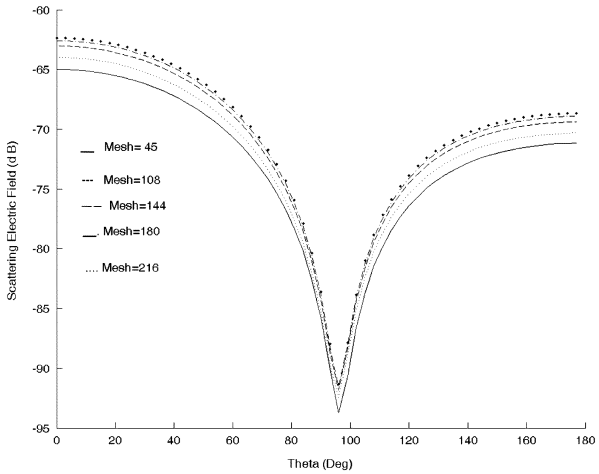

Fig. 6. Scattering field with different meshes.

become increasingly small and it will eventually be close to zero if the frequency is high enough. The frequency at the cross-point between the real and imaginary parts is taken as the lowest resonant frequency.

Fig. 3 shows the comparison between the numerical result and the experimental one. The maximum error between the computational and experimental results is 5.02%.

The results shown in Fig. 4 are obtained with the sensor moving along the Y axis from -0.5 to 0.5 m at 1 kHz and the peak of the waveform is observed to appear above the target. From Figs. 3 and 4, one can see that the computational results match the experimental ones very well.

B. Scattering Field at High Frequency

The following example of FEM-BEM application is to compute the scattering field from a cylinder with its diameter and length both equal to 0.254 m. Its relative permittivity is $\varepsilon_r = 4.0$ and the conductivity is 0.02 S/m.

The incident electric field at 300 MHz is 1 V/m and it comes directly from the Z direction. The cylinder is subdivided into 72 tetrahedrons. The number of unknowns is 197 with the edge-based FEM-BEM algorithm. The number of unknowns is 144 with the method of moment (MoM). The scattering electric field shown in Fig. 5 is computed using the proposed FEM-BEM and MoM algorithms. In the case of homogenous targets, MoM requires less computational time if both methods use the same algorithm in solving linear equations. However, the coefficient matrix of the discretized linear equation of MoM is full and this offsets the advantages of MoM.

On the other hand, one can investigate the accuracy of the solution by computing the relative errors. Unlike [6], $\mathbf{H}$ and $\mathbf{A}_1$ inside the target cannot be calculated together, and therefore the quadratic relative errors [6] cannot be computed. However, we can calculate the scattering electric field with different meshes as shown in Fig. 6. From this figure, one can see that the computational results are closer when the meshes increase. The mean relative error between 180 and 216 meshes is 2.63%.

V. Conclusion

A generalized hybrid method has been proposed and implemented successfully for the 3-D EM computation of EM-I from 10 Hz and the scattering fields at radio frequency. The $\mathbf{H}$–$\mathbf{A}$ model overcomes the shortcomings of traditional mathematical formulations for EM computations. SEEM for general targets has also been derived and applied to interpolate the integral equation while the 3-D EEM is used in differential equations. Finally, the proposed method is applied in several case studies and the errors of the numerical solutions have been investigated. Those results show that the proposed FEM-BEM is valid for wide-band frequency.

Acknowledgment

This work was supported in part by NSFC.

References

[1] J. C. Nedelec, "Mixed finite element in R^3," *Numer. Math.*, vol. 35, pp. 315–341, 1980.
[2] A. Bossavit, "A rational for edge elements in 3-D field computations," *IEEE Trans. Magn.*, vol. 24, no. 1, pp. 74–79, Jan. 1988.
[3] S. Wakao and T. Onuki, "Electromagnetic field computations by the hybrid FE-BE method using edge elements," *IEEE Trans. Magn.*, vol. 28, no. 2, pp. 1487–1490, Mar. 1993.
[4] C. H. Ahn, B. S. Jeong, and S. Y. Lee, "Efficient vectorial hybrid FE-BE method for electromagnetic scattering problem," *IEEE Trans. Magn.*, vol. 30, no. 5, pp. 3136–3139, Sep. 1994.
[5] J. A. Stratton, *Electromagnetic Theory*. New York: McGraw-Hill, 1941, pp. 250–254.
[6] C. Daveau and F. Rioux-Damidau, "New formulation coupling a finite element method and a boundary integral method for the computation of the interaction of waves with a conducting domain," *IEEE Trans. Magn.*, vol. 35, no. 2, pp. 1014–1018, Mar. 1999.
[7] A. Bossavit and I. D. Mayergoyz, "Edge elements for scattering problems," *IEEE Trans. Magn.*, vol. 25, no. 4, pp. 2816–2821, Jul. 1989.
[8] N. Gang, C. B. Baum, and L. Carin, "On the low frequency natural response of conducting and permeable targets," *IEEE Trans. Geosci. Remote Sens.*, vol. 37, no. 1, pp. 347–359, Jan. 1999.

Manuscript received June 20, 2005; revised November 20, 2005 (e-mail: eeslho@polyu.edu.hk).